

Multifocal Vitelliform Paravascular Retinopathy (MVPR)

Weilin Song¹, Sandeep Randhawa², Mark W. Johnson³, Marcela Bohn^{4,5}, Anita Agarwal⁶, Ehsan Rahimy⁷, Kenneth J. Taubenslag^{8,9}, Peter Charbel Issa¹⁰⁻¹², Omar A. Mahroo¹³⁻¹⁴, Jacques Bijon¹⁵, H. Richard McDonald⁶, Scott D. Walter¹⁶, Yoshihiro Yonekawa¹⁷, SriniVas Sadda¹⁸, K. Bailey Freund^{15,19}, David Sarraf^{1,20}

¹ Stein Eye Institute, University of California Los Angeles, CA, USA

² Associated Retinal Consultants, Royal Oak, MI, USA

³ Kellogg Eye Center, University of Michigan, Ann Arbor, MI, USA

⁴ Moorfields Eye Hospital NHS Foundation Trust, London, UK

⁵ West Hertfordshire Teaching Hospital NHS Trust, London, UK

⁶ West Coast Retina Medical Group, San Francisco, CA, USA

⁷ Byers Eye Institute at Stanford, Palo Alto, CA, USA

⁸ VA Maryland Healthcare System, Baltimore VA Medical Center, Baltimore, MD, USA

⁹ University of Maryland, Department of Ophthalmology, Baltimore, MD, USA

¹⁰ Oxford Eye Hospital, Oxford University Hospitals NHS Foundation Trust, Oxford, UK

¹¹ Nuffield Department of Clinical Neurosciences, University of Oxford, Oxford, UK

¹² Department of Ophthalmology, Technical University Munich, Munich, Germany

¹³ NIHR Biomedical Research Centre at Moorfields Eye Hospital and the UCL Institute of Ophthalmology, London, UK

¹⁴ Department of Ophthalmology, St Thomas' Hospital, Westminster Bridge Road, London, UK

¹⁵ Vitreous Retina Macular Consultants of New York, NYH, USA

¹⁶ Retina Consultants P.C., Hartford, Connecticut, USA

¹⁷ Wills Eye Hospital, Mid Atlantic Retina, Thomas Jefferson University, Philadelphia, PA, USA

¹⁸ Doheny Eye Institute, Pasadena, CA, USA; Department of Ophthalmology, University of California-Los Angeles, Los Angeles, CA, USA

¹⁹ Department of Ophthalmology, NYU Grossman School of Medicine, New York, New York, USA

²⁰ Greater Los Angeles VA Healthcare Center, Los Angeles, CA, USA

*Corresponding author

David Sarraf, MD

Department of Ophthalmology

University of California Los Angeles

100 Stein Plaza

Los Angeles, CA 90095

dsarraf@ucla.edu

ABSTRACT

Purpose: To describe a new retinal phenotype characterized by bilateral, multifocal, subretinal vitelliform lesions along the vascular arcades and referred to as multifocal vitelliform paravascular retinopathy or MVPR.

Design: Observational case series.

Methods: Multimodal retinal imaging including color fundus photography, fundus autofluorescence and cross sectional and en-face optical coherence tomography was performed to evaluate and characterize the lesions of MVPR.

Results: Thirteen asymptomatic patients aged 10 to 78 [mean 49 ± 24 , 49% under 50] were evaluated for bilateral retinal lesions. Visual acuity was 20/30 or better at initial evaluation in 22 (85%) eyes and at final follow-up in 14 (70%) of 20 eyes with follow-up. Multifocal small round yellow lesions with distinct borders were identified along the vascular arcades in all patients. The vitelliform lesions were brightly hyperautofluorescent and consisted of focal areas of subretinal hyperreflective material on optical coherence tomography (OCT) that in some cases evolved to hyporeflective spaces with associated hypoautofluorescence. When performed, electroretinography (ERG) and electrooculography (EOG) testing were normal and genetic testing was negative for variants in *BEST1* and other genes associated with vitelliform retinopathies.

Conclusions: MVPR may represent a novel entity of vitelliform disorders with a distinct clinical presentation and phenotype and generally favorable prognosis.

INTRODUCTION

Vitelliform lesions can be associated with a broad spectrum of clinical disorders including inherited and acquired etiologies. Genetic causes include variants in *BEST1*, *PRPH2* and more rarely *IMPG1/2*. Mutations are identified in a minority of vitelliform retinopathies and are typically associated with earlier onset of disease and worse visual prognosis.¹ Acquired vitelliform lesions (AVLs) are associated with a range of etiologies including tractional, paraneoplastic, toxic, exudative, and degenerative disorders.^{2,1}

One proposed unifying pathway in the development of vitelliform lesions across a range of etiologies is loss of photoreceptor (PR)/retinal pigment epithelium (RPE) apposition and impairment of RPE phagocytic function³ leading to the accumulation of degenerating shed PR outer segments in the subretinal space. Trans-differentiation of the RPE and an accrual of RPE organelles, including lipofuscin and melanolipofuscin granules, contribute to these lesions.⁴ The subretinal materials show increased fundus autofluorescence (FAF) and are hyperreflective with optical coherence tomography (OCT).⁵ The main cause of visual morbidity in eyes with vitelliform lesions, which are most commonly found within the macula, is the late occurrence of macular atrophy and less commonly, macular neovascularization.

In this case series of 13 asymptomatic patients, we report a novel phenotype referred to as multifocal vitelliform paravascular retinopathy (MVPR) that is characterized by bilateral, multifocal, round or oval vitelliform lesions predominantly scattered along the major vascular arcades and sparing the fovea.

METHODS

All study-related procedures were performed in accordance with the Declaration of Helsinki, and the Health Insurance Portability and Accountability Act (HIPAA). Investigational Review Board (IRB) approval was obtained commensurate with the requirements of each author's institution. Due to the retrospective nature of the study, informed consent was not required.

Demographic information, pertinent medical and ocular history, visual acuity at presentation and follow-up, and all available diagnostic workup and imaging were collected and reviewed retrospectively. Multimodal retinal imaging was performed and reviewed in each case to best capture the most characteristic features of this novel retinopathy and included widefield color fundus photography, widefield FAF and cross sectional and en face OCT. Subfoveal choroidal thickness was defined as the vertical distance from the hyperreflective line of Bruch's membrane at the fovea to the innermost hyperreflective line of the choroidal-scleral interface. Fluorescein angiography (FA) and indocyanine green angiography (ICGA) were performed in a subset of cases. Full-field electroretinography (ERG), electrooculography (EOG), and mutational analysis were performed in certain cases to rule out Best disease and other genetic causes of vitelliform retinopathy including *PRPH2* and *IMPG1/2*.

Categorical variables were described using frequencies and percentages. Continuous variables were described using means with standard deviations (SD) or medians with interquartile ranges (IQR).

RESULTS

This was an observational case series of 26 eyes from 13 patients, with an unusual pattern of AVLS along the arcades, who were referred for evaluation to various academic centers across the United States and United Kingdom. The average age of our cohort on initial presentation was 49 (SD ± 24) years (49% of our cohort was under 50 years of age) with a range of 10 to 78 years (Table 1). Eight (62%) of the patients were male. More than half of patients were Black (N=8, 62%); three patients were White, one was Hispanic, and one was South Asian. Systemic associations included six (46%) patients with a history of hypertension, three (23%) with hyperlipidemia, two (15%) with type 2 diabetes mellitus (T2DM) without diabetic retinopathy (DR), two (15%) with coronary artery disease (CAD), one (8%) with Lynch syndrome and colon cancer in remission, one (8%) with fibromyalgia, and one (8%) with monoclonal gammopathy of unknown significance (MGUS) and chronic kidney disease (CKD).

Six (46%) patients denied any systemic medications and all patients denied exposure to pentosan polysulfate, deferoxamine, phosphodiesterase inhibitors, checkpoint inhibitors, protein kinase inhibitors, or any other medications known to be associated with vitelliform retinopathy.^{2,6}

Follow up imaging was available for 10 (77%) patients. The median follow-up duration was 17 months with a range from 12 to 108 months. None of the patients reported any visual symptoms attributable to the AVLS at baseline or at final follow-up. Visual acuity was 20/30 or better at initial evaluation in 22 of 26 eyes (85%) and in 14 of (70%) of 20 eyes at final follow-up. One patient was diagnosed with “bilateral optic nerve hypoplasia” at two years of age and exhibited stable hand motion vision from initial evaluation to final follow-up. Another patient showed a decline of vision from 20/30 to 20/40 due to bilateral cataracts after eight years of follow-up. Lastly, one patient presented with visual acuities of 20/70 and 20/60 in the right and left eyes, respectively, that declined to 20/200 in both eyes at final follow-up, four years later, secondary to bilateral retinal vein occlusion, keratoconjunctivitis sicca, and advanced glaucoma.

The phenotype of MVPR was unique and consistent in all 13 patients and clearly differentiated from previously described vitelliform retinopathies with the following characteristic features with multimodal retinal imaging. With widefield (pseudo-) color fundus photography, the small yellow round or oval vitelliform lesions were bilateral and asymmetric and scattered along the major vascular arcades (Figure 1). The subretinal lesions were intensely hyperautofluorescent on FAF and hyperreflective with cross sectional and en-face OCT. Over time, some of the lesions became hypoautofluorescent with a corresponding hyporeflective subretinal space on OCT.

Genetic testing performed in six (46%) patients was negative for mutations in *BEST1*, *PRPH2*, and *IMPG1/2*. One patient had a monoallelic pathogenic mutation in *ABCC6*. Full-field ERG and EOG testing in three (23%) patients was within normal limits. ICGA imaging was performed in three (23%) patients and showed no evidence of choroidal vascular hyperpermeability.

Case 1 (Patient 1 in Table 1)

A 72-year-old asymptomatic Black male with history of T2DM (without DR), HTN, CKD, and MGUS was noted to have multifocal yellowish subretinal lesions scattered along the vascular arcades and in the mid-periphery of both eyes (Figure 2A). Vision was 20/25 right eye (OD) and 20/20 left eye (OS). The lesions were predominantly hyperautofluorescent, with a few lesions along the superior arcade displaying central hypoautofluorescence (Figure 2B). Cross sectional OCT through the hyperautofluorescent lesions showed focal areas of subretinal hyperreflective material that remained stable after six years of follow up (Figure 2C, D), while OCT imaging through the hypoautofluorescent lesions showed hyporeflective subretinal spaces with residual subretinal hyperreflective material (Figure 2E). Baseline subfoveal choroidal thickness was 296 μ m OD and 292 μ m OS. ICGA was not done in this patient. Genetic testing was negative for *BEST1*, *PRPH2* and *IMPG1/2*. Seven years later, the patient remained asymptomatic and the AVLs were largely stable in size, number, and appearance on clinical exam and FAF.

Case 2 (Patient 9 in Table 1)

An asymptomatic 37-year-old South Asian male was referred for evaluation of bilateral retinal lesions detected on routine eye exam. The patient denied any ocular or medical history. Vision was 20/20 OU. Widefield color fundus imaging illustrated multifocal vitelliform lesions distributed along the major vascular arcades and in the mid-periphery with mild vascular tortuosity. The lesions were predominantly hyperautofluorescent and several lesions illustrated associated central hypoautofluorescence (Figure 3A). The lesions stained with FA (Figure 3B) and were hypofluorescent with ICGA (Figure 3C). There was a notable absence of choroidal vascular hyperpermeability in either eye on ICGA. OCT imaging through the lesions illustrated subretinal hyporeflectivity with residual hyperreflective material (Figure 3D). An infectious and inflammatory workup (ACE, QuantiFERON-TB Gold, rapid plasma reagin (RPR) with reflex to RPR and treponemal antibodies, HIV, ANA, and ANCA) was unremarkable.

At the follow-up visit one year later, visual acuity was 20/20 OU. Prior lesions were less hyperautofluorescent with associated attenuation of residual hyperreflective material on OCT (Figure 3E). A new hyporeflective subretinal lesion was noted in the left eye on OCT (Figure 3F, G).

Case 3 (Patient 13 in Table 1)

A 56-year-old asymptomatic White male with medically controlled HTN was referred for evaluation of bilateral retinal lesions. Vision was 20/20 in both eyes (OU). Widefield color fundus imaging illustrated yellow vitelliform lesions along the major vascular arcades in each eye with mild vascular tortuosity. The lesions were brightly hyperautofluorescent (Figure 4A). OCT imaging through the hyperautofluorescent lesions showed subretinal hyperreflective material (Figure 4B-E). Full-field ERG and EOG testing were normal. No mutations were found upon genetic testing for *BEST1*, *PRPH2*, and *IMPG1/2*.

At the time of final follow-up two years later, visual acuity was unchanged at 20/20 OU. Some of the brightly hyperautofluorescent lesions demonstrated progressive hypoautofluorescence with

associated attenuation of the subretinal vitelliform material and the development of RPE atrophy and complete RPE and outer retinal atrophy (cRORA) on OCT OD (Figure 4C, E). Baseline subfoveal choroidal thickness was 420 μm OD and 384 μm OS. ICGA was not performed in this patient.

DISCUSSION

The aim of this report was to describe a novel retinal phenotype characterized by bilateral, round or oval, multifocal vitelliform lesions distributed along the major vascular arcades and sparing the fovea. In several cases, the retinal vessels displayed mild vascular tortuosity and the vitelliform lesions were located preferentially within the curves of the overlying retinal vessels. Most lesions were brightly hyperautofluorescent on FAF and co-localized to a focal area of subretinal hyperreflective material on OCT. Some lesions presented with hypoautofluorescence on FAF corresponding to areas of subretinal hyporefectivity, RPE atrophy, or cRORA on OCT. The lesions stained on FA and were hypofluorescent on ICGA (likely due to blocking of choroidal fluorescence by lipofuscin). Additionally, there was no evidence of choroidal vascular hyperpermeability with ICGA.

When performed, ERG and EOG testing were within normal limits. Mutational analysis did not reveal genetic causes of vitelliform dystrophy such as variants in *BEST1*, *PRPH2*, and *IMPG1/2*. Monoallelic mutations in *ABCC6*, detected in one patient in our cohort, can be associated with a spectrum of retinal alterations including reticular pseudodrusen,⁷ while biallelic *ABCC6* mutations are associated with pseudoxanthoma elasticum but this mutation is unlikely to explain the vitelliform lesions in this patient. Other causes of acquired vitelliform lesions such as vitreoretinal traction, age-related macular degeneration (AMD) (i.e. large drusen and subretinal drusenoid deposits), retinal toxicity, paraneoplastic and autoimmune retinopathy were excluded by multimodal imaging and by history.

Out of 13 eyes with available measurements, increased subfoveal choroidal thickness on OCT (greater than $\geq 300 \mu\text{m}^8$) was found in three eyes. Patients with pachychoroid can develop hyperautofluorescent pachydrusen at the level of the RPE.⁹ The MVPR lesions described in our series were larger, rounder, more intensely and more uniformly hyperautofluorescent, and without exception were clustered in the paravascular retina. Pachyvitelliform maculopathy (PVM) is another recently described entity in elderly patients with pachychoroid without drusen or subretinal drusenoid deposits (SDD).¹⁰ Patients with PVM typically exhibit central foveolar vitelliform lesions that are

predominantly unilateral. None of our cases exhibited foveolar lesions, all were bilateral, and half of the patients were under 50 years of age. None of the cases in our series were associated with exudative complications of pachychoroid disease such as serous pigment epithelial detachment (PED). Additionally, there was no evidence of choroidal hyperpermeability or neovascularization on ICGA to suggest an exudative process.

All AVLs were distributed along the major vascular arcades which can be a region of increased vitreoretinal (VR) traction.¹¹ However, cross-sectional OCT showed no evidence of focal VR traction overlying the vitelliform lesions or along the neighboring vessels. Additionally, en-face OCT ruled out subtle signs of VR traction such as paravascular inner retinal defects in ten (77%) cases.¹¹

One important pathophysiological mechanism of vitelliform lesion development is impaired phagocytosis of PR outer segments by RPE cells, resulting in accumulation of modified proteins and lipids within RPE cells and the subretinal space.³ This impairment in RPE phagocytic function may occur in the setting of genetic mutations (resulting in impaired lipid transport or lipofuscin overload in the RPE cells), inflammation, cellular senescence (resulting in loss of RPE polarity and RPE atrophy), and loss of apposition between PRs and RPE cells due to tractional or exudative processes.² The clinical phenotype of MVPR is distinct from Best disease and other forms of inherited vitelliform maculopathy, and no patients in this series were found to have potentially pathogenic mutations. None of the patients in this series exhibited evidence of intraocular inflammation or active malignancy to suggest a paraneoplastic disease process. The wide age distribution of our population makes it unlikely that these lesions are the result of RPE senescence. Although there was no evidence of anteroposterior VR traction identified with OCT, we hypothesize that the paravascular location of the MVPR lesions and the association with vascular tortuosity may indicate the presence of occult tangential VR traction.

Vitelliform lesions can remain stable for many years, as was the case with most lesions in this study. However, some vitelliform lesions can eventually progress to incomplete and complete RPE and outer retinal atrophy (iRORA, cRORA),⁴ indicative of RPE dysfunction, impairment and decline.

Several lesions in this case series were hyporeflective or frankly atrophic (i.e. iRORA/cRORA) with OCT at baseline or at the final follow up visit.⁵ We hypothesize that newly acquired MVPR lesions are initially hyperautofluorescent and may eventually progress to a more hypoautofluorescent phenotype as a result of lipofuscin clearance and/or progressive RPE atrophy. None of the patients in this series reported any visual symptoms or vision loss that could be attributed to the lesions, likely due to the eccentricity of the lesions from the fovea.

Limitations of this study include the small study size and variable diagnostic workup and follow-up duration. A total of four patients completed genetic testing and three underwent electrophysiology testing to rule out Best disease and other genetic etiologies of vitelliform dystrophy. There is no clear etiology for the localization of the lesions to the major vascular arcades, and although the distribution is very atypical for classic Best disease, multifocal Best disease or autosomal recessive bestrophinopathy (ARB) may be a consideration in the other seven (58%) patients who did not receive genetic or electrophysiological testing. However, the absence of macular findings such as intraretinal and central subretinal fluid would be exceedingly unusual for ARB.^{12,13} Although two patients (17%) endorsed a history of cancer, none had active metastatic disease, making paraneoplastic acute exudative polymorphous vitelliform maculopathy (AEPVM) unlikely. The relatively inert and stable time course of most MPVR lesions and lack of central macular involvement is also atypical for AEPVM.^{14,15}

In conclusion, this case series highlights a novel phenotype referred to as MVPR and characterized by asymptomatic paravascular vitelliform lesions that largely spare the fovea. The most typical vitelliform lesions in MVPR are yellowish in color and brightly hyperautofluorescent. Some lesions exhibit central hypoautofluorescence. On OCT, most lesions demonstrate subretinal hyperreflective material suggestive of extracellular lipofuscin accumulation and some lesions can progress to a focal area of subretinal hyporeflectivity and/or RPE atrophy. Further studies to characterize the natural history of MVPR within a larger patient cohort are warranted. Future studies

should also aim to confirm the potential association of MVPR with other clinical features including African American ancestry, vascular tortuosity, and pachychoroidopathy.

ACKNOWLEDGEMENTS AND FINANCIAL DISCLOSURES

A. Funding/Support: This work was generously supported by an unrestricted Research to Prevent Blindness grant. This material is also the result of work supported with resources and the use of facilities at the VA Maryland Health Care System, Baltimore MD. The contents do not represent the views of the U.S. Department of Veterans Affairs or the United States Government.

B. Financial Disclosures:

- W. Song: None
- S. Randhawa: None
- M. Johnson: Serves on Independent Data Monitoring Boards for Aura Biosciences and Opthea (not related to the current work).
- M. Bohn: None
- A. Agarwal: None
- E. Rahimy: Regeneron (C, F), Genentech (C, F), Apellis (C,F), Iveric (C,F), Abbvie (C,F), Zeiss (C)
- K. Taubenslag: None
- P. Charbel Issa: Heidelberg Engineering (research support)
- O. Mahroo: Janssen (Advisory Board)
- J. Bijon: None
- H. R. McDonald: None
- S. Walter: Speaker for Apellis, Bausch & Lomb, Genetech/Roche, Regeneron, and Spark Therapeutics. Consultant for Alimera/EyePoint Pharmaceuticals, Allergan, Astellas/Iveric Bio, Bausch & Lomb, Castle Biosciences, Genetech/Roche, Ideaya Biosciences, Lupin, Novartis, and Regeneron. (None relevant to the current work).
- Y. Yonekawa: Alcon (C), EyePoint (C), Genentech/Roche (R), Kodiak (R), Regeneron (R)
- S. Sadda: Consultant (C): 4DMT, Abbvie, Alexion, Allergan Inc., Alnylam Pharmaceuticals, Amgen Inc., Apellis Pharmaceuticals, Inc., Astellas, Bayer Healthcare Pharmaceuticals, Biogen MA Inc., Boehringer Ingelheim, Carl Zeiss Meditec, Catalyst Pharmaceuticals Inc., Centervue Inc., GENENTECH, , Heidelberg Engineering, Hoffman La Roche, Ltd., Iveric Bio, Janssen Pharmaceuticals Inc., Nanoscope, Notal Vision Inc., Novartis Pharma AG, Optos Inc., Oxurion/Thrombogenics, Oyster Point Pharma, Regeneron Pharmaceuticals Inc., Samsung Bioepis, Topcon Medical Systems Inc., EyePoint, OTX, Neurotech; Financial Support (F): Carl Zeiss Meditec, Optos, Heidelberg, Nidek, iCare, Roche
- K. B Freund: Consultant (C): Apellis Pharmaceuticals, Carl Zeiss Meditec, Genentech, Heidelberg Engineering, Novartis, & Regeneron
- D. Sarraf: Amgen (C, F, R), Avecida (C), Annexon (C), Bayer (C, R), Boehringer (F), Eidon/Centervue (R), Genentech (C, F, R), Ocuphire (C), Visionix/Optovue (F, I, C, S).

C. Other acknowledgements: The authors would like to acknowledge Avery Freund for his contribution to this manuscript and specifically related to the selection of the optimal name for this novel phenotype.

REFERENCES

1. Chowers I, Tiosano L, Audo I, Grunin M, Boon CJF. Adult-onset foveomacular vitelliform dystrophy: A fresh perspective. *Prog Retin Eye Res.* 2015;47:64-85. doi:10.1016/j.preteyeres.2015.02.001
2. Iovino C, Ramtohul P, Au A, et al. Vitelliform maculopathy: Diverse etiologies originating from one common pathway. *Surv Ophthalmol.* 2023;68(3):361-379. doi:10.1016/j.survophthal.2023.01.009
3. Arnold JJ, Sarks JP, Killingsworth MC, Kettle EK, Sarks SH. Adult vitelliform macular degeneration: a clinicopathological study. *Eye.* 2003;17(6):717-726. doi:10.1038/sj.eye.6700460
4. Brinkmann M, Bacci T, Kar D, et al. Histology and clinical lifecycle of acquired vitelliform lesion, a pathway to advanced age-related macular degeneration. *Am J Ophthalmol.* 2022;240:99-114. doi:10.1016/j.ajo.2022.02.006
5. Freund KB, Laud K, Lima LH, Spaide RF, Zweifel S, Yannuzzi LA. ACQUIRED VITELLIFORM LESIONS: Correlation of Clinical Findings and Multiple Imaging Analyses. *RETINA.* 2011;31(1):13. doi:10.1097/IAE.0b013e3181ea48ba
6. Hsu ST, Ponugoti A, Deaner JD, Vajzovic L. Update on Retinal Drug Toxicities. *Curr Ophthalmol Rep.* 2021;9(4):168-177. doi:10.1007/s40135-021-00277-x
7. Gliem M, Wieg I, Birtel J, et al. Retinal findings in carriers of monoallelic ABCC6 mutations. *Br J Ophthalmol.* 2020;104(8):1089-1092. doi:10.1136/bjophthalmol-2018-313448
8. Lee K, Ra H, Lee JH, Baek J, Lee WK. Classification of Pachychoroid on Optical Coherence Tomographic En Face Images Using Deep Convolutional Neural Networks. *Transl Vis Sci Technol.* 2021;10(7):28. doi:10.1167/tvst.10.7.28
9. Spaide RF. DISEASE EXPRESSION IN NONEXUDATIVE AGE-RELATED MACULAR DEGENERATION VARIES WITH CHOROIDAL THICKNESS. *Retina Phila Pa.* 2018;38(4):708-716. doi:10.1097/IAE.0000000000001689
10. Hilely A, Au A, Lee WK, et al. Pachyvitelliform maculopathy: an optical coherence tomography analysis of a novel entity. *Br J Ophthalmol.* Published online July 13, 2023. doi:10.1136/bjo-2022-322553
11. Romero-Morales VA, Bousquet E, Abraham N, et al. EVALUATION OF PARAVASCULAR INNER RETINAL DEFECTS USING EN FACE OPTICAL COHERENCE TOMOGRAPHY. *RETINA.* 2023;43(10):1644. doi:10.1097/IAE.0000000000003889
12. Kim HR, Han J, Kim YJ, et al. Clinical Features and Genetic Findings of Autosomal Recessive Bestrophinopathy. *Genes.* 2022;13(7):1197. doi:10.3390/genes13071197
13. Birtel J, Gliem M, Herrmann P, MacLaren RE, Bolz HJ, Charbel Issa P. Peripapillary Sparing in Autosomal Recessive Bestrophinopathy. *Ophthalmol Retina.* 2020;4(5):523-529. doi:10.1016/j.oret.2019.12.008
14. Barbazetto I, Dansingani KK, Dolz-Marco R, et al. Idiopathic Acute Exudative Polymorphous Vitelliform Maculopathy: Clinical Spectrum and Multimodal Imaging Characteristics. *Ophthalmology.* 2018;125(1):75-88. doi:10.1016/j.ophtha.2017.07.020
15. Chan CK, Gass JDM, Lin SG. Acute exudative polymorphous vitelliform maculopathy syndrome. *Retina Phila Pa.* 2003;23(4):453-462. doi:10.1097/00006982-200308000-00002

FIGURE LEGENDS

Figure 1. Montage color fundus photography and wide-field fundus autofluorescence (FAF) of all 13 patients included in this case series. Note the consistent characteristic findings of each patient with MVPR (multifocal vitelliform paravascular retinopathy), namely round, yellow, hyperautofluorescent vitelliform lesions clustered around the major arcades with or without vascular tortuosity.

Figure 2. 72-year-old black male with multifocal vitelliform paravascular retinopathy (MVPR). (A) Color fundus photography shows round, yellow multifocal lesions along the vascular arcades and outside the foveal region. (B) Vitelliform lesions are hyperautofluorescent with wide-field fundus autofluorescence (FAF). (C-E) Optical coherence tomography (OCT) through the hyperautofluorescent lesions show corresponding subretinal hyperreflective vitelliform material that remains stable after six years of follow up. OCT through the hypoautofluorescent lesions show subretinal hyporeflective spaces.

Figure 3. 37-year-old south Asian male with multifocal vitelliform paravascular retinopathy (MVPR). (A) Bilateral lesions are predominantly hyperautofluorescent on fundus autofluorescence (FAF), while some lesions display a hypoautofluorescent center. (B) Fluorescein angiography (FA) of the vitelliform lesions shows patchy window defects with late staining. (C) Indocyanine green (ICG) shows corresponding focal areas of hypofluorescence with no evidence of leakage. (D, E) Optical coherence tomography (OCT) through the lesions shows subretinal hyporeflective spaces with hyperreflective vitelliform material that is reabsorbed at follow up. (F, G) At follow-up over a year later, OCT shows a new subretinal lesion within the left eye.

Figure 4. 56-year-old white male with multifocal vitelliform paravascular retinopathy (MVPR). (A) Bilateral lesions are hyperautofluorescent on fundus autofluorescence (FAF), while few lesions

display hypoautofluorescence. (B-E) After two years of follow-up, some lesions display decreased autofluorescence. Optical coherence tomography (OCT) through the hyperautofluorescent lesions show subretinal hyperreflective vitelliform material and OCT through the hypoautofluorescent lesions show complete retinal pigment epithelium (RPE) and outer retinal atrophy (cRORA). Lesions with loss of hyperautofluorescence on follow-up show evidence of reabsorption of vitelliform material and new-onset RPE atrophy and cRORA on OCT.

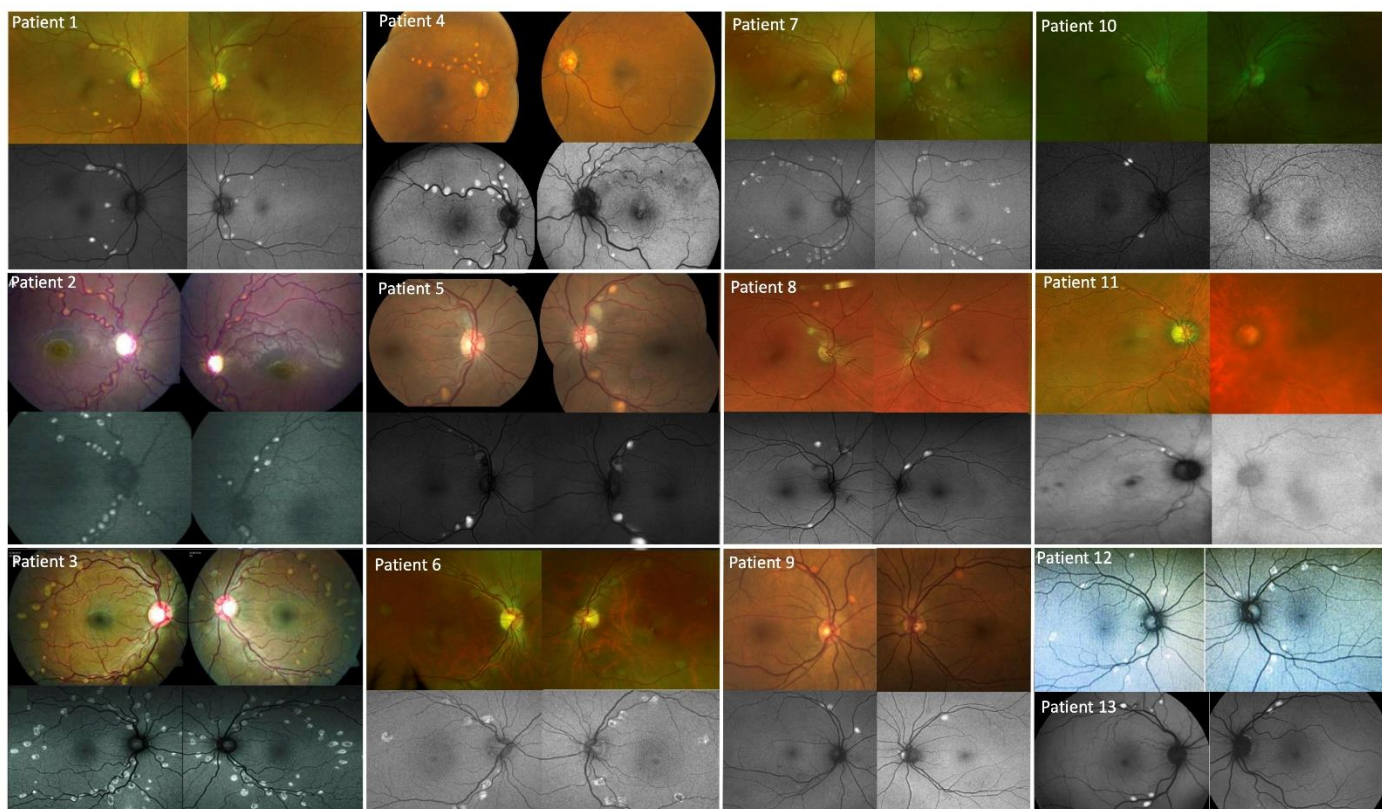


Figure 1

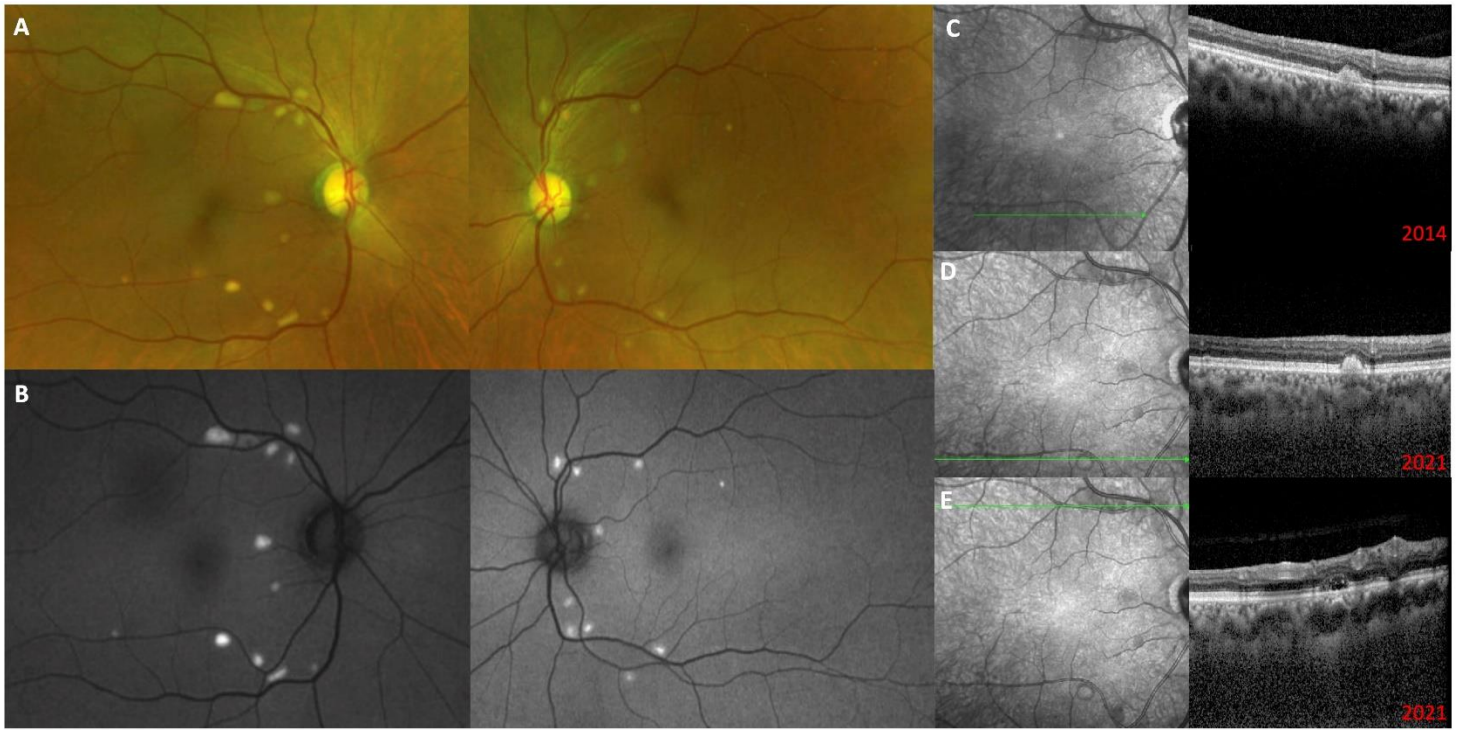


Figure 2

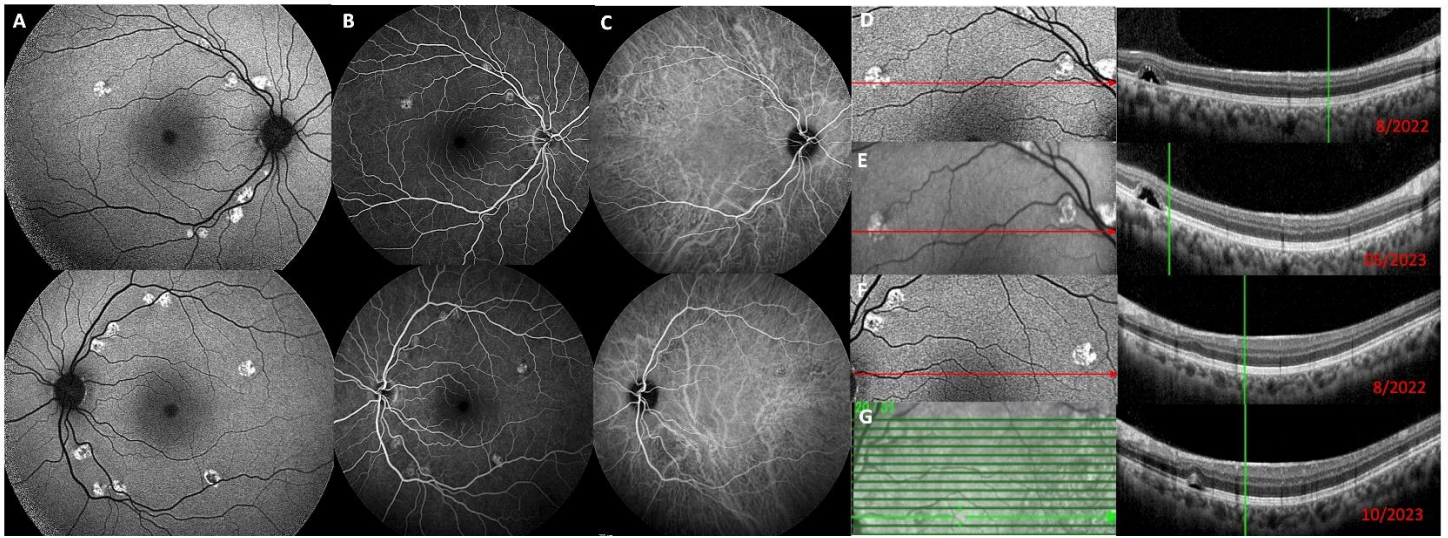


Figure 3

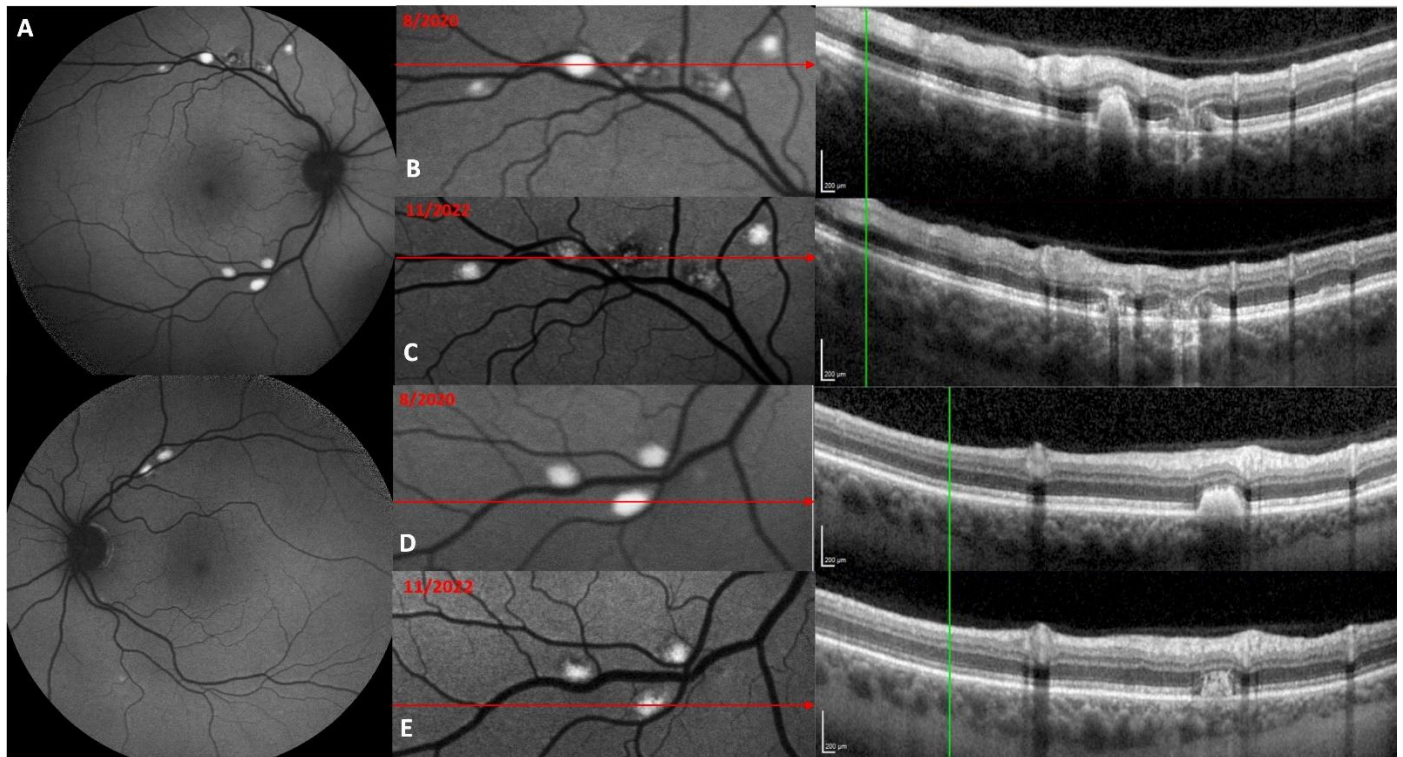


Figure 4

Patient	Age	Gender	Ethnicity	PMH	Meds	Ocular hx	Initial Vision OD	Initial Vision OS	Follow up Duration (months)	Follow up Vision OD	Follow up Vision OS	Color fundus findings	FAF findings	OCT findings	SFCT OD (µm)	SFCT OS (µm)	Additional workup
1	72	M	Black	DM s DR, MGUS, CKD	Metformin	Cataracts	20/25	20/20	108	20/25	20/20	Bilateral multifocal yellow lesions along vascular arcades and posterior pole.	Lesions are mostly hyperautofluorescent with some central hypoautofluorescence.	Mixed subretinal hyperreflective material with hyporeflective spaces.	296	292	IMPG1/IMPG2/BEST 1/RDS genetic testing (negative)
2	10	F	Black	None	None	"Bilateral optic nerve hypoplasia", nystagmus at age 2	HM	HM	-	HM	HM	Bilateral multifocal yellow lesions along vascular arcades with tortuous vasculature.	Lesions are mostly hyperautofluorescent with some central hypoautofluorescence.	Mixed subretinal hyperreflective material with hyporeflective spaces.	-	-	Genetic testing for BEST1 and PRPH2 (negative); ICGA (no leakage)
3	32	M	Black	None	None	None	20/20	20/20	12	20/20	20/20	Bilateral multifocal yellow lesions along vascular arcades and posterior pole with tortuous vasculature.	Lesions are mostly hyperautofluorescent with some central hypoautofluorescence.	Predominantly hyporeflective spaces.	-	-	Serum electrophoresis, IMPG1/IMPG2/BEST 1/RDS genetic testing (negative), full field ERG and EOG (normal)
4	68	F	Black	HTN, HLD	Losartan, hydrochlorothiazide	Cataracts	20/30	20/30	96	20/40	20/40	Bilateral multifocal yellow lesions along vascular arcades and posterior pole with tortuous vasculature.	Lesions are mostly hyperautofluorescent.	Predominantly subretinal hyperreflective material.	-	-	ANA, RF, ACE, lysozyme, ANCA, ESR, CRP, CBC unremarkable
5	59	F	Black	HTN, T2DM, Lynch syndrome w/ colon cancer s/p colectomy and chemo, in remission	None	None	20/20	20/20	20	20/20	20/20	Bilateral multifocal yellow lesions along vascular arcades and posterior pole with mildly tortuous vasculature.	Lesions are mostly hyperautofluorescent.	Predominantly subretinal hyperreflective material.	-	-	Full body scans - no cancer recurrence. Declined genetic testing/ERG/EOG
6	50	F	Black	Fibromyalgia, OA	None	None	20/20	20/20	9	20/20	20/20	Bilateral multifocal yellow lesions along vascular arcades.	Lesions are mostly hyperautofluorescent with some central hypoautofluorescence.	Mixed subretinal hyperreflective material with hyporeflective spaces.	-	247	ERG/EOG (normal)
7	17	M	Black	None	None	None	20/20	20/20	-	-	-	Bilateral multifocal yellow lesions along vascular arcades and posterior pole.	Lesions are mostly hyperautofluorescent with some central hypoautofluorescence.	Predominantly hyporeflective spaces.	224	214	ICGA, FA (no leakage)
8	74	M	White	HTN, CAD, HLD	Rosuvastatin, ezetimibe, valsartan, loratadine, aspirin, duloxetine	CEIOL OU	20/20	20/20	-	-	-	Bilateral multifocal yellow lesions along vascular arcades and posterior pole.	Lesions are mostly hyperautofluorescent with some central hypoautofluorescence.	Both lesions with subretinal hyperreflective material and hyporeflective spaces present.	297	263	Declined genetic testing
9	67	M	White	HTN, HLD, BPH	Finasteride, tamsulosin	None	20/20	20/20	-	-	-	Bilateral multifocal yellow lesions along vascular arcades and posterior pole.	Lesions are primarily hyperautofluorescent.	Predominantly subretinal hyperreflective material.	200	257	Genetic testing with single mutation in ABCC6
10	37	M	South Asian	None	None	None	20/20	20/20	14	20/20	20/20	Bilateral multifocal yellow lesions along vascular arcades and posterior pole.	Lesions are mostly hyperautofluorescent with some central hypoautofluorescence.	Predominantly hyporeflective spaces.	245	233	ACE, quant gold, syphilis, HIV, ANA/ANCA (unremarkable); ICGA (no leakage)
11	78	F	Black	CAD, HTN, uterine cancer s/p	Aldactone, Apresoline, Aspirin, Entresto,	CRVO OD, BRVO OS (Eylea	20/70	20/60	48	20/200	20/200	Bilateral multifocal yellow lesions along	Lesions are mostly hyperautofluorescent.	Predominantly hyperreflective spaces.	313	282	None

				hysterectomy	HCTZ, Lasix, Lipitor, Losartan, Metoprolol	OU); advanced POAG OU, ERM OD s/p PPV/MP						vascular arcades, tortuous vessels, optic nerve with cupping					
12	20	M	Hispanic	None	None	None	20/20	20/20	12	20/20	20/20	Not available	Lesions are mostly hyperautofluorescent with some central hypoautofluorescence.	Predominantly hyporeflective space.	-	-	ERG/EOG (normal)
13	56	M	White	HTN	Amlodipine, bisoprolol, doxazosin, ramipril, tegretol	None	20/20	20/20	36	20/20	20/20	Not available	Lesions are mostly hyperautofluorescent with some hypoautofluorescence.	Mixed regions with subretinal hyperreflective material and RPE atrophy.	420	384	ERG, EOG (negative). IMPG1/IMPG2/BEST 1/RDS genetic testing (negative)

Table 1. Clinical history and imaging findings for all patients included.

PMH=past medical history; DM=diabetes mellitus; DR=diabetic retinopathy; MGUS=monoclonal gammopathy of unknown significance; CKD=chronic kidney disease; HTN=hypertension; HLD=hyperlipidemia; OA=osteoarthritis; CAD=coronary artery disease; BPH=benign prostatic hyperplasia; HCTZ=hydrochlorothiazide; CEIOL=cataract extraction with intraocular lens implantation; CRVO=central retinal vein occlusion; BRVO=branch retinal vein occlusion, POAG=primary open angle glaucoma; ERM=epiretinal membrane; PPV=pars-plana-vitrectomy; MP=membrane peel; HM=hand motion; FAF=fundus autofluorescence; OCT=optical coherence tomography; RPE=retinal pigment epithelium; SFCT=subfoveal choroidal thickness; ICGA= indocyanine green angiography; ERG=electroretinography; EOG=electrooculography; FA=fluorescein angiography; ANA=antinuclear antibody; RF=rheumatoid factor; ACE=angiotensin converting enzyme; ANCA=antineutrophilic cytoplasmic antibody; ESR=erythrocyte sedimentation rate; CRP=C-reactive protein; CBC=complete blood count